Physica C: Superconductivity and its applications 528 (2016) 27–34

Contents lists available at ScienceDirect

Physica C: Superconductivity and its applications

journal homepage: www.elsevier.com/locate/physc

Superconductivity in MgB_2 irradiated with energetic protons

Viorel Sandu[a,*], Liviu Craciun[b], Alina Marinela Ionescu[a,c], Gheorghe Aldica[a], Lucica Miu[a], Andrei Kuncser[a,c]

[a] National Institute of Materials Physics, 405A Atomistilor Str, Magurele, 077125 Romania
[b] Horia Hulubei" National Institute of Nuclear Physics and Engineering, 30 Reactorului str., Magurele, 077125 Romania
[c] University of Bucharest, Faculty of Physics, 405 Atomistilor Str, Magurele, 077125 Romania

ARTICLE INFO

Article history:
Received 14 March 2016
Revised 26 June 2016
Accepted 7 July 2016
Available online 9 July 2016

Keywords:
MgB_2
Proton irradiation
Critical current
Pinning energy
Magnetic relaxation
Flux jump

ABSTRACT

A series of MgB_2 samples were irradiated with protons of 11.3 and 13.2 MeV. Magnetization data shows an insignificant reduction of the critical temperatures but a continuous decrease of the Meissner fraction with increasing fluence or energy. All samples show a consistent improvement of the critical current density compared to the virgin sample and an increase of the pinning energy at high fields as resulted from relaxation data.

1. Introduction

Current transport in superconductors is related to the formation of efficient pinning centers that should prevent the motion of flux lines. In the race for creation of artificial pinning centers, particle irradiation was successfully used, mainly in high temperature superconductors, MgB_2 included [1–14]. Particle irradiation creates vacancies and interstitials (Frenkel pairs-FP) in excess of equilibrium concentration both in the magnesium and boron sublattices. The FP have a permanent tendency toward recombination and/or aggregation and, eventually, creation of dislocation structures. That tendency is facilitated by the thermal energy which stimulates the migration of defects through the crystal. However, a rather high concentration of vacancies always exists in MgB_2 due to the facile loss of Mg during fabrication [16,17]. They constitute strongly biased sinks for further absorption of other vacancies. These sinks and the uneven kinetic of interstitials and vacations favor the nucleation of the point defect loops and, further, the growth of dislocations and other defects generated by the release of the associated strains. Actually, only these extended defects are efficient pinning centers in the case of MgB_2 because it has a longer coherence length, $\xi \sim 10$ nm. The isolated point defects, which are effective in cuprate superconductors, are practically inactive in this case. However, the defects, no matter the way they are created, have influence on the electronic properties of the material, hence, on the superconducting characteristics. That fact happens because the superconducting MgB_2 phase is close to the structural instability, which depends on electron concentration, a concentration which is easy altered by structural defects [17]. First, disorder reduces the electron mean free path, hence, decreases the coherence length and increases the upper critical field H_{c2} [18]. Second, it couples the π-band and the σ-band by interband scattering which diminishes both the superconducting gaps [15] and critical temperature T_c [19].

These aspects were well investigated for neutron irradiated MgB_2 [1–6] but there is a shortage of data regarding the effect of the damages created by protons irradiation. By our knowledge, the effect of proton irradiation on different superconducting properties were investigated only with protons of energy between 0.4 and 7 MeV [7–9,20–22] and the results are somehow contradictory. For example, using protons up to 6 MeV and fluences below 10^{16} p cm^{-2}, Mezzeti et al. [8], claimed that effects on transport properties are almost negligible whereas significant effects were reported at low temperatures with protons of 2 [7] and 3 MeV [22] energy. However, the sample structures, which are different, put their fingerprint on the field and temperature dependence of the superconducting and transport characteristics.

This paper presents the effect of high energy protons, above 10 MeV, on the superconducting properties of MgB_2. In this way,

* Corresponding author. Tel.: +40212418152; fax: +40213690177.
E-mail address: vsandu@infim.ro (V. Sandu).

http://dx.doi.org/10.1016/j.physc.2016.07.006
0921-4534/

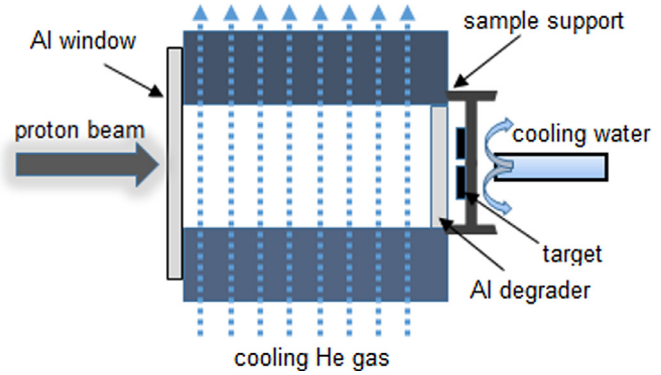

Fig. 1. Experimental setup for proton irradiation.

we extend the range of proton energy which has not been explored yet. The reason is that, at higher energy, the distance traveled by protons, i.e., the *range*, increases, as well as the energy loss along the range. Therefore, the probability to find concentration of defects along the range, hence, in a certain way, correlated defects, is high though the energy loss is non uniform. Consequently, the longer the range, the higher the capability to fix a vortex line. However, there is a limitation in the energy due to the induced radioactivity. That process usually occurs for protons with energy much higher than 10 MeV but the problem is not critical for materials made of low Z elements like MgB_2 which have short half-lives in order of minutes or hours.

2. Experimental

High density pellets of MgB_2 were prepared by spark plasma sintering (SPS) technique from commercial MgB_2 powder (Alfa Aesar). A carbon die with MgB_2 powder was placed in the SPS equipment, heated up to 1150 °C with a pulsed current which was increased in time up to 1400 A average value. During the heating, a pressure of about 95 MPa was applied. After dwelling for about 3 min at the final temperature, the sample was cooled down to room temperature. Detailed data on the process are presented elsewhere [23].

The as prepared polycrystalline MgB_2 batch had a mass density higher than 90% of the ideal density. Pellets cut from the batch (targets) were mounted on aluminum supports and submitted to proton irradiation. The irradiation set up is shown in Fig. 1. A proton beam of 14 MeV energy from a Cyclotron TR 19 accelerator enters through a pure aluminum foil of 50 μm thickness, crosses the He cooling channel and hits the target. In order to reduce the proton energy, degraders made of pure aluminum of different thickness were mounted in the front of the sample. The sample support is cooled with flowing water. The energy loss through aluminum window and degrader, and, subsequently, the energy of the final beam was calculated using the SRIM (Stopping and Range of Ions in Matter) code [24]. The fluence of protons Φ was calculated from the current-time diagram (Fig. 2) as $\Phi = (eS)^{-1}\int_0^{t_{max}} I(t)dt$, where e is the proton charge, S the transversal area of the proton beam, $I(t)$ is the current and t_{max} the total time of irradiation. A sample, P1, was irradiated with more energetic protons, 13.2 MeV, whereas the rest of the samples were irradiated at 11. 3 MeV but at different fluences. The irradiation data for each sample are presented in the Table 1

Simulation by means of a SRIM code for the penetration depth of the 11.3 MeV and 13.2 MeV protons in MgB_2 gave about 730 and 960 μm, respectively (Fig. 3) which is slightly longer than the sample thickness. Consequently, practically the entire sample volume is affected by irradiation.

The as-prepared samples were investigated by transmission electron microscopy using a JEM-ARM200F analytical electron microscope. Data on magnetic properties were collected using a SQUID (MPMS-Quantum Design) magnetometer at different temperatures and in sweeping fields. DC relaxation measurements were taken in a time window $t_w \sim 5 \times 10^3$ s with the relaxation time t was considered to be zero when magnet charging was finished.

3. Results and discussion

3.1. Sample microstructure and morphology

Fig. 4 shows the micrographs of the virgin sample in Z-contrast image. In addition to large MgB_2 grains, nanoparticles of MgO are present at the grain boundaries and also small amounts of higher borides (Fig. 4a and Fig. 4b). The later were identified as MgB_4 by X-ray diffraction. They result from the high temperature decomposition of MgB_2 in the presence of the residual oxygen and formation of MgO and MgB_4. We expect that these nanoparticles should play the role of sinks for defect accumulation. After irradiation, there is a noticeable increase of the density of MgO nanoparticles although they have smaller sizes. That increase was attributed to the residual oxygen in the irradiation room which reacts with the Mg released as the sample warms up under proton fluence (Fig. 4c). The high resolution micrograph (Fig. 4d) shows the presence of many less ordered areas, defect wells, spread throughout the structure. The role of these defect wells is to release the strain accumulated by the creation of the dislocations and accommodate crystalline nanodomains [25]

3.2. Magnetization

The temperature T dependence of the magnetic susceptibility χ is shown in Fig. 5 for both virgin and irradiated samples. The critical temperature is slightly affected by irradiation. The suppression is maximal, i.e., $\Delta T_c = -0.6$ K, for the sample P1 which was irradiated with proton of 13.4 MeV, the highest energy in our experiment. That negligible decrease suggests that Frenkel pairs do not lead to interband scattering. Band computation related to Mg vacancies showed that the generated holes go to both σ and π bands. In the σ-band, the holes remain delocalized, hence, the T_c is not influenced. The holes in the π−band present a certain degree of localization [26] but they cannot affect severely the critical temperature. These results are in agreement to point contact Andreev reflection data [27]. Our results also confirm data on single crystalline samples [8,9,21,22]. Despite the insignificant shift of the critical temperature, the diamagnetic signal, hence, the superconducting volume fraction, notably decreases in the case of irradiated sample, a decrease with reaches more than 20 % in the case of the sample P1. Actually, the decrease is of the same order for all irradiated samples. That is compatible with a microscopic phase separation in superconducting and nonsuperconducting regions [26,28]. The same sample shows both the most reduced superconducting screening, as resulted from the zero field cooling (ZFC) branch and the most reduced Meissner fraction (See the inset to Fig. 5). The Meissner fraction f_M was obtained from the field cooled (FC) magnetization by reporting it to the ideal susceptibility ($\chi_0 = 1/4\pi$). f_M is a measure of the pinning of vortices, specifically, it was shown that f_M decreases with increasing the flux pinning parameter $\gamma_{c1} \sim \frac{J_c(T_{c1})L}{H_{c1}(T_{c1})}$ [29]. Here, J_c is the critical current density, L the sample size, H_{c1} the lower critical field, and T_{c1} is the temperature at which the applied field H is equal to H_{c1}. As the inset to Fig. 5 shows the Meissner fraction decreases for all irradiated samples. Thus, the decrease of f_M is of 67 and 65 % for the samples P1 and P2, respectively, and smaller for the samples P3